JOURNAL OF SOLID STATE CHEMISTRY **131,** 298–304 (1997)
ARTICLE NO. SC977380

Alluaudite-like Structure of the Complex Arsenate $NaCaCdMg_2(AsO_4)_3$

S. Khorari, A. Rulmont, and P. Tarte

Institut de Chimie, Université de Liège, B-4000, Sart Tilman par Liège 1, Belgium

G. Miehe

Fachbereich Materialwissenschaft, TH Darmstadt Petersenstr. 20, D-6100 Darmstadt, Germany

D. Antenucci

Laboratoire de Minéralogie, Université de Liège B-4000, Sart Tilman par Liège 1, Belgium

and

B. Gilbert

Laboratoire de Chimie Analytique et Electrochimie, Université de Liège, Institut de Chimie B6, B-4000, Sart Tilman par Liège 1, Belgium

Received March 5, 1997; accepted March 6, 1997

The existence of a continuous series of solid solutions $NaCaCdMg_2[(PO_4)_{1-x}(AsO_4)_x]_3$ ($0 \leq x \leq 1$) suggests an alluaudite-like structure of the arsenate $NaCaCdMg_2(AsO_4)_3$. This is definitely confirmed by a Rietveld analysis of its X-ray powder diffractogram. The crystal cell is monoclinic, space group $C2/c$, with $a = 12.2363(1)$, $b = 12.9869(1)$, $c = 6.7742(1)$ Å, $\beta = 113.7985(3)^\circ$. The Mg^{2+} cations are essentially located on the $M(2)$ sites of the alluaudite structure, but the distribution of the Na^+, Ca^{2+}, and Cd^{2+} cations over the $M(1)$, $X(1)$, and $X(2)$ sites is more or less disordered. The existence of a partial disorder in the cation distribution is supported by some diffuseness of the Raman and IR spectra.

INTRODUCTION

The alluaudite structure has been first determined on natural minerals with a fairly complex chemical composition (1). Substantial progress in our knowledge of the crystal chemistry of this family was realized through the synthesis of a series of complex phosphates such as $Na_2M_2^{2+}M^{3+}(PO_4)_3$ ($M^{2+} = Mg, Mn, Cd$; $M^{3+} = In, Ga, Fe, Cr$) (2) and $NaCaCdMg_2(PO_4)_3$ (3). This last composition is particularly interesting since it is the first reported case of a phosphate alluaudite completely free from trivalent cations. We have accordingly investigated the possible existence of the corresponding arsenate $NaCaCdMg_2(AsO_4)_3$ and of the intermediate compositions $NaCaCdMg_2[(PO_4)_{1-x}(AsO_4)_x]_3$.

EXPERIMENTAL

Synthesis of the Compounds

Although these compounds can be prepared by conventional solid state reaction techniques, better results are obtained by first reacting the stoichiometric quantities of the necessary reagents ($NaHCO_3$, $CaCO_3$, $CdCO_3$, MgO, $NH_4H_2PO_4$, As_2O_3—all of analytical purity) with an excess of pure, concentrated nitric acid. The resulting solution is evaporated to dryness; the dry residue is transferred into a covered Pt crucible which is progressively heated up to a final temperature of 800–900°C. This temperature is maintained with intervening mixing and grinding until no change is observed in the X-ray powder diffraction diagram (generally a few days).

X-Ray Diffraction

X-ray powder diffractograms were recorded with either a Philips diffractometer (Fe$K\alpha$ radiation) or a Siemens D-5000 diffractometer (Cu$K\alpha$ radiation), with either Si or $Pb(NO_3)_2$ as external standards. Unit cell parameters were refined with the INDLSQ least square program.

0022-4596/97 $25.00

TABLE 1
Experimental Details for the Rietveld Refinement

2θ range ($CuK\alpha_1$)	9°–100°
Step width	0.02°
Number of reflections	511
Refined parameters	
Structural parameters	
Positional	27
Population	4
Thermal (atomic displ.)	20
	51
Cell parameters[a]	4
Profile	7
Preferred orientation (1 0 −2)	1
Zero-point (2θ)	1
Scale factor	1
	65

[a] Cell parameters: 12.2363(1) Å, 12.9869(1) Å, 6.7742(1) Å, $\beta = 113.7985(3)$ °.

Accurate X-ray diffraction data for Rietveld refinement were collected on a STOE-STADI powder diffractometer equipped with a rotating transmission holder, using germanium-monochromatized $CuK\alpha$ radiation. The experimental details for the Rietveld refinement are given in Table 1.

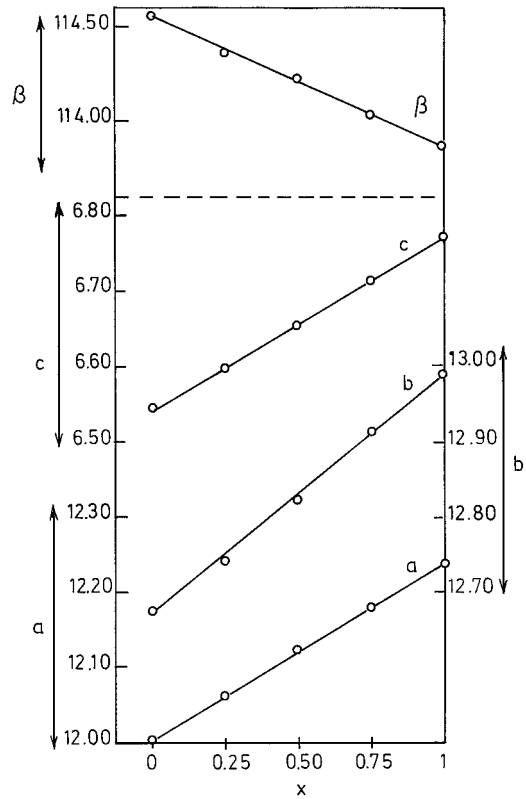

FIG. 1. Variations of the unit cell parameters of the solid solutions $NaCaCdMg_2[(PO_4)_{1-x}(AsO_4)_x]_3$.

Vibrational Spectra

The IR spectra were recorded with a Beckman 4250 spectrometer (2000–300 cm^{-1}; KBr disks) and a Polytec FIR 30 interferometer (350–30 cm^{-1}; polyethylene disks).

The Raman spectra were recorded with a Coderg double monochromator equipped with an Ar^+ laser (laser power 200–300 mW on the 514.5 nm green line; slit width about 3 cm^{-1}).

Differential Thermal Analysis

The experiments were carried out with a Fisher DTA equipment, using heating and cooling rates of 600° hr^{-1}.

RESULTS

X-Ray Diffraction

From its X-ray powder diffractogram, it is immediately evident that unlike $NaCa_2Mg_2(AsO_4)_3$ (4), the arsenate $NaCaCdMg_2(AsO_4)_3$ is not a garnet-like phase. On the other hand, some analogies are noticed with the diffractogram of the corresponding phosphate although important differences appear in the small-angle region. This difficulty has been solved by the study of the intermediate compositions $NaCaCdMg_2[(PO_4)_{1-x}(AsO_4)_x]_3$ with $x = 0.25, 0.50$, and 0.75.

The diffractogram of the $x = 0.25$ composition is fairly easily indexed by comparison with that of the pure

TABLE 2
Positional and Isotropic Thermal Parameters and Site Occupancy

Site	Wyckoff position	x	y	z	$B_{eq.}$ (Å^2)
$X(1)$[a]	4*b*	0	1/2	0	1.35(12)
$X(2)$[a]	4*e*	0	−0.0255(3)	1/4	1.73(13)
$M(1)$[a]	4*e*	0	0.2648(1)	1/4	1.11(8)
$M(2)$[a]	8*f*	0.2793(2)	0.6574(2)	0.3647(5)	0.80(8)
As(1)	4*e*	0	−0.2820(1)	1/4	0.80(5)
As(2)	8*f*	0.2335(1)	−0.1077(1)	0.1293(2)	0.85(4)
O(1)	8*f*	0.4563(4)	0.7050(4)	0.5304(7)	0.8(1)
O(2)	8*f*	0.1004(4)	0.6340(4)	0.2285(8)	1.4(1)
O(3)	8*f*	0.3310(4)	0.6667(3)	0.1120(7)	0.6(1)
O(4)	8*f*	0.1173(4)	0.4120(4)	0.3067(7)	0.9(1)
O(5)	8*f*	0.2265(4)	0.8205(4)	0.3309(8)	0.9(1)
O(6)	8*f*	0.3402(4)	0.5050(4)	0.3942(7)	0.9(1)

[a] See Table 3.

TABLE 3
Two Possible Cation Distributions on the *X* and *M* Sites

Model 1: *R*, 3.36%; R_w, 4.59%; *R*(Bragg), 2.56%; GOF, 1.52								sum
X(1)		*X*(2)		*M*(1)		*M*(2)		Na + Ca + Cd + + 2 Mg = 103 el.
Ca	Cd	Na	Ca	Na	Cd	Mg	Cd	
0.686(3)	0.314	0.640(10)	0.360	0.410(3)	0.590	0.976(2)	0.024	Na 1.05(1)
28.8(1) el.		14.2(1) el.		32.8(1) el.		(2×) 12.9(1) el.		Ca 1.05(1)
								Cd 0.95(1)
								Mg 1.95(1)
								101.6 el.
Model 2: *R*, 3.36%; R_w, 4.59%; *R*(Bragg), 2.60%; GOF, 1.52								Na 1.18(1)
X(1)		*X*(2)		*M*(1)		*M*(2)		Ca 0.88(1)
								Cd 0.99(1)
Na	Cd	Na	Ca	Ca	Cd	Mg	Cd	Mg 1.95(1)
								101.6 el.
0.532(3)	0.468	0.646(13)	0.354	0.526(4)	0.474	0.976(2)	0.024	
28.3(1) el.		14.2(1) el.		33.3(1) el.		(2×) 12.9(1) el.		

phosphate, and this indexation can be extended to the other compositions, including the pure arsenate. For every composition, all diffraction peaks are satisfactorily accounted for by a monoclinic cell, the reflection conditions being those of the $C2/c$ space group. Figure 1 shows that the variations of the unit cell parameters with composition are practically linear.

A Rietveld refinement of the arsenate compound has been carried out to confirm the alluaudite-like structure and to get some information about the distribution of the cations

TABLE 4
Interatomic Distances (Å) and Angles (°) (Corresponding Values for the Phosphate in Brackets)

X(1)–O(4)	2.297(4) (2×)	[2.29]	*X*(2)–O(6)	2.429(4) (2×)	[2.40]
X(1)–O(2)	2.324(5) (2×)	[2.31]	*X*(2)–O(6)	2.545(3) (2×)	[2.57]
X(1)–O(4)	2.569(4) (2×)	[2.54]	*X*(2)–O(1)	2.700(6) (2×)	[2.58]
X(1)–O(2)	3.122(4) (2×)	[3.11]	*X*(2)–O(3)	3.134(5) (2×)	[3.07]
Mean	2.578	[2.56]	*X*(2)–O(5)	(3.280(5) (2×))	[2.66]
			Mean	2.702	
M(1)–O(3)	2.283(4) (2×)	[2.27]	*M*(2)–O(2)	2.026(4)	[2.00]
M(1)–O(1)	2.306(4) (2×)	[2.34]	*M*(2)–O(3)	2.054(5)	[2.07]
M(1)–O(4)	2.328(4) (2×)	[2.33]	*M*(2)–O(1)	2.091(4)	[2.05]
M(1)–O(2)	(3.245(5) (2×))		*M*(2)–O(6)	2.096(5)	[2.09]
Mean	2.305	[2.31]	*M*(2)–O(5)	2.111(5)	[2.11]
			M(2)–O(5)	2.199(5)	[2.23]
			Mean	2.096	[2.09]
As(1)–O(1)	1.690(5) (2×)	[1.53]	O(1)–As(1)–O(1)	107.5(3)	[106.4]
As(1)–O(2)	1.693(4) (2×)	[1.54]	O(1)–As(1)–O(2) (2×)	106.8(2)	[107.1]
Mean	1.692	[1.54]	O(1)–As(1)–O(2) (2×)	118.3(2)	[116.3]
			O(2)–As(1)–O(2)	99.7(2)	[104.0]
			Mean	109.5	[109.5]
As(2)–O(5)	1.684(5)	[1.54]	O(5)–As(2)–O(3)	112.2(2)	[111.1]
As(2)–O(3)	1.686(5)	[1.55]	O(5)–As(2)–O(6)	110.9(2)	[111.1]
As(2)–O(6)	1.693(5)	[1.52]	O(5)–As(2)–O(4)	106.0(2)	[106.9]
As(2)–O(4)	1.717(3)	[1.57]	O(3)–As(2)–O(6)	106.2(2)	[107.3]
Mean	1.692	[1.55]	O(3)–As(2)–O(4)	110.3(2)	[109.1]
			O(6)–As(2)–O(4)	111.5(2)	[111.5]
			Mean	109.5	[109.5]

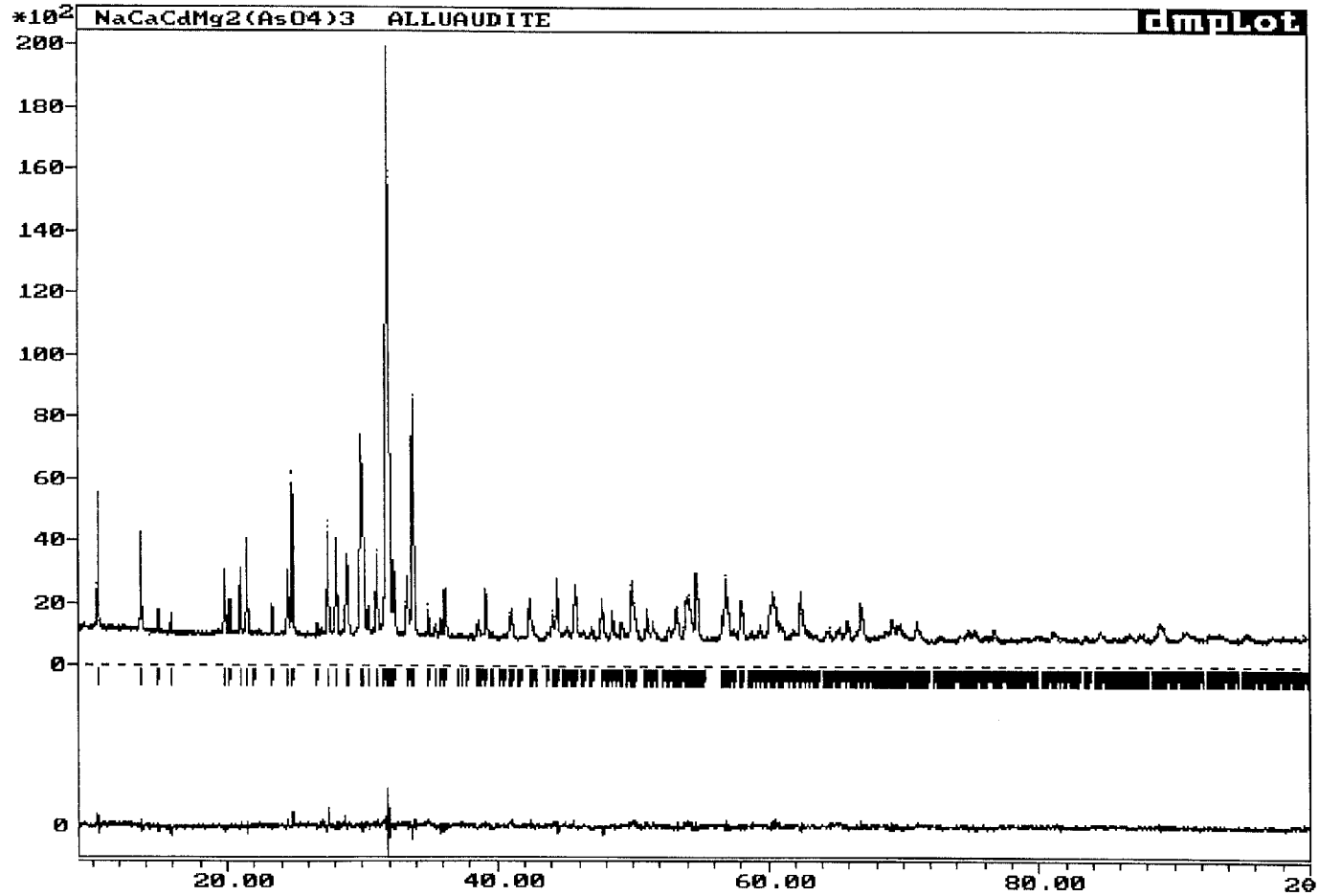

FIG. 2. Final Rietveld plot for $NaCaCdMg_2(AsO_4)_3$. The upper trace shows the observed data as dots and the calculated pattern is shown by the solid line. The lower trace is a plot of the difference: observed minus calculated. The vertical markers show the positions calculated for Bragg reflections.

on the different sites of this structure. The results of this refinement are presented in Tables 1 (unit cell parameters), 2 (positional and isotropic thermal parameters and site occupancy), 3 (possible cation distributions), and 4 (interatomic distances and angles) and in Figs. 2 and 3.

It became clear very soon in the course of refinement that $X(1)$, $X(2)$, and $M(1)$ cannot be occupied by a single species of cations. By its coordination as well as by its scattering power, $M(2)$ seemed to be identified as a pure Mg site. The preliminary result of the refinement expressed in electrons per site was: $X(1)$, 28.5; $X(2)$, 14.5; and $M(1)$, 32.7. Since for $X(1)$ and $M(1)$ these numbers are greater than 20 (= Ca), the sites *must* contain Cd. Since for $X(2)$ the number is less than 20, $X(2)$ *must* contain Na.

Under the auxiliary conditions that

(A) merely two atomic species share in one site, and

(B) $M(2)$ is Mg,

only two distributions of cations are possible:

$X(1) = (Ca, Cd)$, $X(2) = (Na, Ca)$, $M(1) = (Na, Cd)$, $M(2) = Mg$ (model 1) or

$X(1) = (Na, Cd)$, $X(2) = (Na, Ca)$, $M(1) = (Ca, Cd)$, $M(2) = Mg$ (model 2).

(If Cd would go to $X(2)$ instead of Ca, 100% of Ca had to go to one site (otherwise condition (A) would be violated), which does not match the observed electron densities.)

Although the dependence of the normalized scattering factors on $\sin\theta/\lambda$ is different for Na, Ca and Cd, both models are indistinguishable by Rietveld refinement. For both models, the sum of electrons in $X(1)$, $X(2)$, and $M(1)$ refines to 75.7(2) which is less than 79 (= 1 Na + 1Ca + 1Cd). The use of scattering curves for Na^+, Ca^{2+}, and Cd^{2+} does not change this situation and makes the agreement factors worse. When the population parameter of $M(2)$ is given free for refinement, it increases to 1.075(7) for both models with a significant decrease in the R factors. If $M(2)$ is partially occupied by Cd which, for crystal chemical reasons, is the most probable substitution, a ratio Cd : Mg = 0.025:0.975 is obtained. The auxiliary condition (B) is only slightly violated, and the sum of electrons of all X and M sites which should be 103 refines to 101.6(2) for

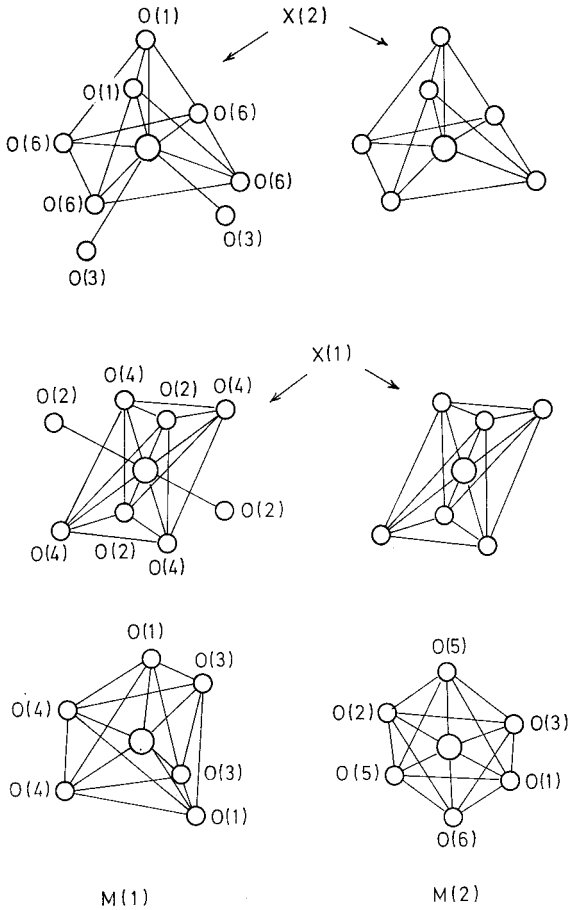

FIG. 3. Coordination polyhedra of the $X(2)$, $X(1)$, $M(1)$, and $M(2)$ sites. For the $X(2)$ and $X(1)$ sites, the coordination is shown with or without the long X–O distance of about 3.12 Å, thus illustrating the $6 + 2$ coordination of these cations.

both models. (During these calculations, the electron density scale is fixed by the As and O atoms which together represent 72% of the scattering power.)

Besides the sum of electrons, the calculated ratio of cations is an additional criterion for the consistency of the result. As shown in Table 3, model 1 is clearly favored by this criterion.

The considerations above are based on the unproven assumption that auxiliary condition (A) is correct. The electron excess at the $X(2)$ site shows that this condition is not strictly valid and 2.5% Mg must be distributed over the other sites. Nevertheless, it is reasonable that the large cations Na and Ca occupy the largest crystallographic site $X(2)$.

As already pointed out by Moore (1), it is not easy to describe the coordination sphere around $X(1)$, $X(2)$, and $M(1)$. If we discard the two very long distances of 3.280 Å ($X(2)$–O(5)) and 3.245 Å ($M(1)$–O(2)), the coordination is eightfold for $X(1)$ and $X(2)$ and sixfold for $M(1)$ (Table 4). But, as illustrated by Fig. 3, we could also consider, for $X(1)$ and $X(2)$, a sixfold coordination with two additional oxygen anions at about 3.12 Å ($X(1)$–O(2) and $X(2)$–O(3)). A typical octahedral coordination is observed for $M(2)$ only (Fig. 3). These results are in agreement with the published data on the alluaudite structure (1, 3, 5) and we can conclude that the results of the Rietveld refinement support an alluaudite-like structure for the arsenate $NaCaCdMg_2(AsO_4)_3$, with the Mg^{2+} cations essentially located on the $M(2)$ crystal sites. The distribution of the other cations on the remaining crystallographic sites must be partially disordered.

Vibrational Spectra

The IR and Raman spectra of $NaCaCdMg_2(AsO_4)_3$ are represented in Fig. 4. As we have already pointed out (5), the low symmetry of the structure precludes a detailed assignment of the bands. The stretching frequencies of the $(AsO_4)^{3-}$ anion are observed in the 950–750 cm^{-1} region: as usual, the essential contribution to the IR spectrum comes from the v_3 antisymmetric motions; the Raman spectrum exhibits one strong peak and weak shoulders which, after deconvolution (Fig. 5), appear as three bands of strong (854 cm^{-1}) or medium (829 and 881 cm^{-1}) intensity and one very weak component at 794 cm^{-1}. It seems reasonable to assign the three bands of strong or medium intensity to the three components which, according to a factor group analysis (6), are issued from the split v_1 vibrations of the $AsO_4(1)$ ($1A_g$) and $AsO_4(2)$ ($1A_g + 1B_g$) ions. The very weak band at 794 cm^{-1} would be one of the components of the v_3 vibrations.

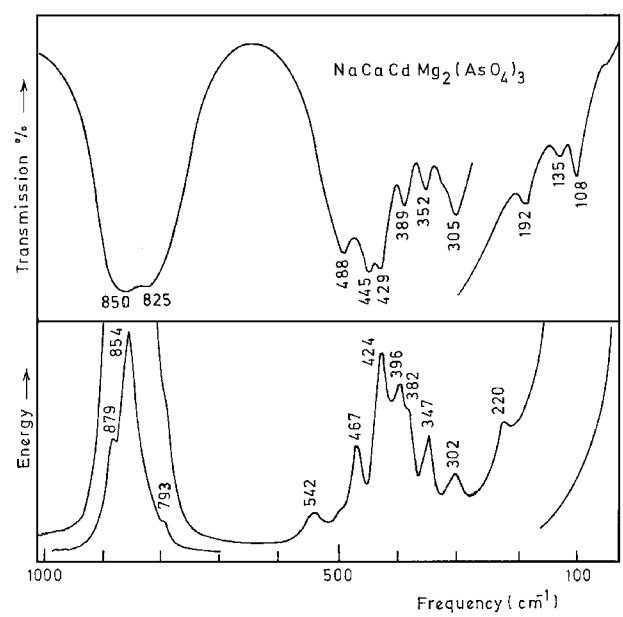

FIG. 4. IR (upper) and Raman (lower) spectrum of $NaCaCdMg_2(AsO_4)_3$.

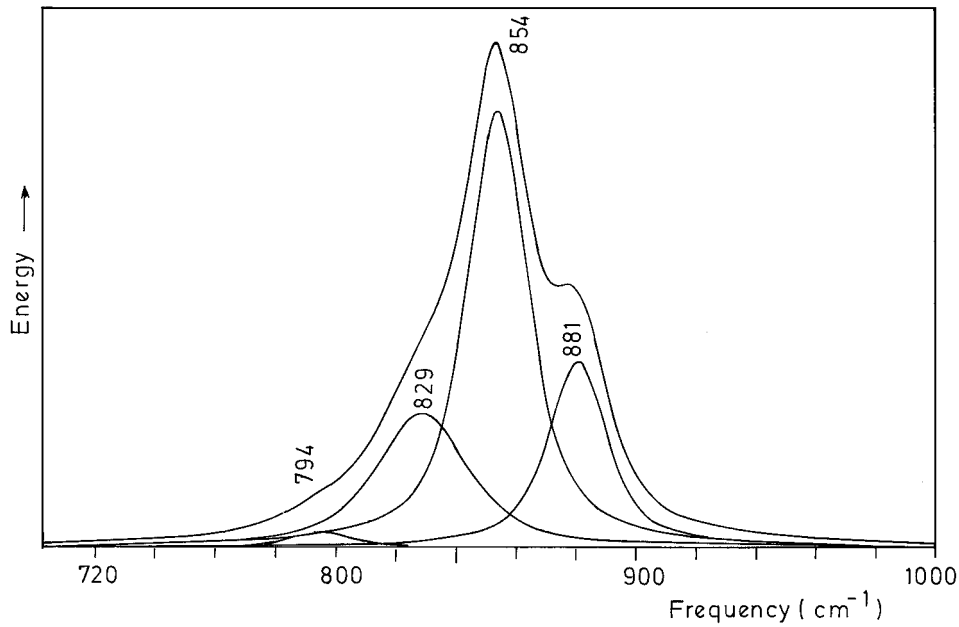

FIG. 5. Raman spectrum of $NaCaCdMg_2(AsO_4)_3$: the 1000–700 cm^{-1} region after deconvolution.

The bending vibrations are observed in the 550–350 cm^{-1} region, but the existing results do not allow a discrimination between the symmetric (ν_2) and the antisymmetric (ν_4) vibrations, which fall in the same frequency range (see, e.g., (7)). Likewise, no clear-cut limit can be traced between the low-frequency part of the $(AsO_4)^{3-}$ bending vibrations and the high-frequency part of the lattice vibrations (librational motions of the anions; translational motions of the anions and cations). Translational frequencies of the Mg^{2+} cation in octahedral sites have been evidenced in the 350–300 cm^{-1} region of the IR spectrum of the metaborate $Ba_2Mg(B_3O_6)_2$ (8) and at 283 cm^{-1} in the IR spectrum of $KMgP_3O_9$ with the benitoite structure (9). These data suggest that the 305 cm^{-1} band (Fig. 4) is mainly due to a translation of Mg^{2+} in the $M(2)$ octahedral site of the alluaudite-like arsenate. This assignment is supported by the fact that a similar band is observed at 337 cm^{-1} in the IR spectrum of the corresponding phosphate (3), and at 329, 318, and 309 cm^{-1} in the spectra of the solid solutions $NaCaCdMg_2[(PO_4)_{1-x}(AsO_4)_x]_3$ with $x = 0.25$, 0.50, and 0.75, respectively.

No definite assignment can be proposed for the very low-frequency IR bands observed below 200 cm^{-1}.

Another point to be considered is the existence, in the spectra, of some diffuseness which becomes more conspicuous by comparison with the spectrum of another alluaudite-like compound such as $NaCdIn_2(PO_4)_3$ (5). This diffuseness, which is only moderate, is the result of the partial disorder in the cationic distribution of Na^+, Ca^{2+}, and Cd^{2+} cations over the $X(2)$, $X(1)$, and $M(1)$ sites.

Thermal Behavior

No event is observed in the DTA diagram, up to 1050°C (the upper limit of our DTA equipment), and no significant change is observed in either X-ray diffractogram or vibrational spectrum of the sample recovered after the DTA experiment. The compound is thus stable up to 1050°C, at least for a short time. This behavior is different from that of the corresponding phosphate, which exhibits a polymorphic (slowly reversible) transformation into a fillowite structure at 854°C (10). This transition is no longer observed in the solid solutions $NaCaCdMg_2[(PO_4)_{1-x}(AsO_4)_x]_3$, even for $x = 0.25$. For this latter composition, melting without decomposition is observed at 1022°C.

DISCUSSION

Cation–Oxygen Distances in the Phosphate and in the Arsenate

The values in Table 4 show that the increase in the unit cell volume (984.96 $Å^3$ for the arsenate against 906.02 $Å^3$ for the phosphate) is essentially due to the increase in the size of the tetrahedral group ($\bar{d}_{As-O} \simeq 1.69$ Å; $\bar{d}_{P-O} \simeq 1.54$ Å), whereas the other cation–oxygen distances remain approximately constant. Nevertheless, we notice a small (but probably significant) increase in the mean $X(2)$–O and $X(1)$–O distances (corresponding to the weakest bonds of the structure), whereas the distances remain constant (within the limits of the experimental error) for the more strongly bonded $M(1)$ and $M(2)$ cations.

We can also notice the remarkable correspondence between the distortion of the ideal geometry of the PO_4 and AsO_4 tetrahedra obtained from two independent refinements.

Cationic Composition of Some Arsenates and Alluaudite versus Garnet Structure

The existing data are very scarce, but they suggest that relatively small modifications of the chemical composition may lead to either a garnet or an alluaudite structure.

In the present case, the replacement of one Ca by one Cd cation is sufficient to suppress the garnet–alluaudite polymorphism existing in $NaCa_2Mg_2(AsO_4)_3$ (6) and to preserve only the alluaudite structure in $NaCaCdMg_2(AsO_4)_3$.

Likewise, the garnet structure of natural berzeliite (ideally $NaCa_2Mg_2(AsO_4)_3$, with some Mn^{2+} replacing a bivalent cation) is replaced by an alluaudite structure when some Ca^{2+} is replaced by Pb^{2+}, as in the mineral caryinite (11).

It would be premature to try to deduce, from these two examples, the reasons for the garnet–alluaudite transformation: both Cd^{2+} and Pb^{2+} cations are able to occupy the dodecahedral sites of the garnet structure (12); the changes in ionic radii are small to moderate and go in opposite directions (the Cd^{2+} cation is slightly smaller than, but the Pb^{2+} cation is somewhat larger than, the Ca^{2+} cation). Finally, the type of electronic structure remains which could be a determining factor. It is clear that a broader pattern of experimental data is necessary to progress in this matter, and we are now exploring new arsenate compositions which could lead to either a garnet or an alluaudite structure.

ACKNOWLEDGMENTS

The authors thank the FNRS and the Research Council of the University of Liège for their financial support for the acquisition of the D5000 Siemens diffractometer. S.K. is particularly grateful to the FNRS for a travel grant. S.K. thanks Professor J. Choisnet and Dr. F. Archaimbault for their valuable help and discussions in the Rietveld calculations.

REFERENCES

1. P. B. Moore, *Am. Mineral.* **56,** 1955 (1971).
2. D. Antenucci, Doctorate Thesis, University of Liège, 1992.
3. D. Antenucci, A. M. Fransolet, G. Miehe, and P. Tarte, *Eur. J. Mineral* **7,** 175 (1995).
4. H. Schwarz and L. Schmidt, *Z. Anorg. Allg. Chem.* **382,** 257 (1971).
5. D. Antenucci, G. Miehe, P. Tarte, W. Schmahl, and A. M. Fransolet, *Eur. J. Mineral* **5,** 207 (1993).
6. S. Khorari, A. Rulmont, R. Cahay, and P. Tarte, *J. Solid State Chem.* **118,** 267 (1995).
7. H. Siebert, "Anwendungen der Schwingungsspektroskopie in der anorganischen Chemie." Springer–Verlag, Berlin, 1966.
8. A. Rulmont, P. Tarte, and M. Almou, *Spectrochim. Acta A* **49,** 1695 (1993).
9. P. Tarte, A. Rulmont, K. Sbai, and M. H. Simonot-Grange, *Spectrochim. Acta A* **43,** 337 (1987).
10. D. Antenucci, G. Miehe, P. Tarte, and A. M. Fransolet, Communication presented at the "Journées de la Société Française de Minéralogie-Cristallographie, Marseille"; *Bull. Soc. Franç. Min. Crist.* **5**(2), 27 (1993). [Abstract]
11. P. J. Dunn and D. R. Peacor, *Miner. Mag.* **51,** 281 (1987).
12. S. Geller, *Z. Kristallog.* **125,** 1 (1967).